Co-Robotic Ultrasound Imaging System

600.446. Advanced Computer Integrated Surgery
Spring 2017
Johns Hopkins University, Baltimore, MD

Group 7: Ting-Yun Fang, Weiqi Wang
Mentors: Haichong Kai Zhang, Dr. Russ H. Taylor,
Dr. Emad M. Boctor

1 Introduction

Ultrasound imaging is widely used in medical diagnosis. It has several advantages including lower cost, greater accessibility, and non-invasiveness. However the limitation of ultrasound imaging are: low resolution, highly depends on sonographer's experience, and difficult to reproduce throughout radiation treatments or operators. In addition, sonographers often suffer from musculoskeletal pain and repetitive strain injuries because many ultrasound-scanning applications require them to apply a large force with bizarre a body gesture.

To overcome these obstacles, robotic ultrasound technology has been developed. Sen et al. integrated a robotic arm with US system through cooperative control and implemented virtual fixture constraints for guidance of reproducing US image [1]. Hennersperger et al. developed a 7 degree-of-freedom (DOF) robotic US system for autonomous US scanning [2]. Another novel application, named as synthetic tracked aperture ultrasound imaging system (STRATUS) can be found in Zhang et al.'s work [3]. This method uses a robotic arm to track the US imaging coordinate and integrates it with synthetic aperture algorithm; it improves the US image resolution especially for deep region focusing and increases the field of view.

In this project, we aimed to integrate STRATUS with an existing power steering robotic US system [4]. This system combines a robotic arm, UR5, dual force sensors and US system. With cooperative control, the robot follows operator's motion and is able to differentiate the user's force input and the contact force between US probe

and tissue. Incorporating STRATUS into the power steering system could maximize the use of robotic arm, extending the current system to more applications.

2 Project Overview

To integrate STRATUS with current cooperatively controlled robotic US system, virtual fixture is essential. Because STRATUS implementation needs the US probe align with a specific direction and orientation, virtual fixture constraints the user's motion and ensures the consistency of imaging coordinate. Our project first implemented several virtual fixtures for the UR5 using constraint method [5] and virtual spring method [6][7], and validated the US robotic system with phantom study, animal and human experiment. Also, we improved the efficiency of the previous STRATUS program, developed real time STRATUS visualization; and designed an upgraded version of the US attachment.

3 Material and Methods

3.1 System Overview

The project is built up on an existing system developed in previous research (Figrue 1) [4]. The co- robotic US system includes a 6-DOF robot arm (UR5, Universal Robots, Odense, Denmark), a 6-DOF force/torque sensor (FT-150, Robotiq) mounted on the robot's end effector, a detachable US attachment with a contact force sensor (Model 31 Mid, Honeywell).

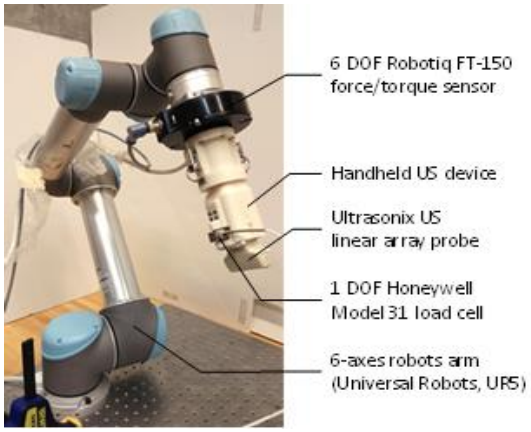

Figure 1. The co-robotic US system built in the previous research [4].

3.2 Admittance Robot Control:

In this research, we are using cooperative control. The robot would follow user's motion based on the 6-DOF force sensor's reading. The advantage of cooperative control is that the robot is always under the control of user. It is easier for the operator to adapt with the new system because the handling process is similar with the conventional US acquisition procedure. The mathematical formula follows the admittance robot control equation:

$$\dot{x}_t = K \cdot (F_t + \gamma F_c) = \mathrm{diag}(K_1, K_2, \cdots, K_6) \cdot (F_t + \gamma F_c) \tag{1}$$

$$\dot{x}_w = Ad_{gwt} \dot{x}_t \tag{2}$$

where $\dot{x}_t$ and $\dot{x}_w$ are the target tool velocity with respect to (w.r.t.) the robot tip frame and the world frame, respectively; Ad_{gwt} is the adjoint transformation from the top frame to the world frame; $F_t = [Fx, Fy, Fz, Mx, My, Mz]^T$ denotes the human handling force and torque, measured by the 6 DOF sensor w.r.t. the robot tip frame; $F_t = [0, 0, Fc, 0, 0, 0]^T$ is the contact force obtained from the 1 DOF load cell. K and $\gamma \in [0,1]$ are the constant admittance gain and force scaling factor, respectively, which were empirically defined. The force applied by an operator's hand is magnified by the robot based on this force scaling factor γ.

3.3 Virtual Fixture Implementation:

Two distinct methods were applied in the robot system to accomplish virtual fixture. The first method is a constrained method for virtual fixture, introduced for human-machine collaborative systems (HMCS) [5]. This method is based on the optimized constrained control and can be applied to multiple scenarios.

3.3.1 Constraints Method for Virtual Fixture

Virtual fixtures can be represented a geometric constraints, which can be applied in a quadratic optimization problem with linear constraints. The governing equation is:

$$\arg\min_{\frac{\Delta q}{\Delta t}} \left\| W\left(\frac{\Delta \vec{x}}{\Delta t} - \frac{\Delta \vec{x}_d}{\Delta t}\right) \right\| \tag{3}$$

$$s.t. \quad \frac{H\Delta \vec{x}}{\Delta t} \geq \vec{h}$$

$$\left(\frac{\Delta \vec{x}}{\Delta t} - \frac{\Delta \vec{x}_d}{\Delta t}\right) = J\left(\frac{\Delta \vec{q}}{\Delta t}\right)$$

where Δq is the desired incremental motions of the joint variables, $\Delta \overrightarrow{x_d}$ and $\Delta \vec{x}$ are the desired and the computed incremental motions of the task variables in Cartesian space. J is the Jacobian matrix mapping task space to joint space. W is a weighting diagonal matrix. Δt is the time interval of control loop. This system is built upon the assumption that the incremental motions in each iterated loop is small enough that the Jacobian approximation is accurate.

3.3.1.1 Stay On Line

A basic constraint that can be appropriate for ultrasound imaging is to move along a reference line in 3D, which can allow the STRATUS algorithm to receive the most relevant series of images. Given a line $L(s) = \overrightarrow{L_0} + \hat{l} \cdot s$, where $\overrightarrow{L_0}$ is a point on the line and $\hat{l}$ is the unit vector indicating the direction of the line. While the virtual fixture is active, the system must correct any offset from its current position to the closest point on line, and each increment motion must be along or close to the line. If

we name $\overrightarrow{\delta_p}$ as the perpendicular vector from the tool tip to the line, it can be determined by

$$\vec{\delta}_p = \vec{x}_p - \vec{P}_{cl} \tag{4}$$

where $\overrightarrow{x_p}$ is the tool position, and $\overrightarrow{P_{cl}}$ is the closest point on plane.

To perform this computation, a rotation matrix that transforms the plane to the world coordinate frame is needed. To determine R_3, we use the following equations:

$$R_3 = \left[\widehat{v_1}\widehat{v_2}\hat{l}\right];\ \widehat{v_1} = \frac{\hat{l} \times \hat{l'}}{\|\hat{l} \times \hat{l'}\|};\ \widehat{v_2} = \frac{\widehat{v_1} \times \hat{l}}{\|\widehat{v_1} \times \hat{l}\|} \tag{5}$$

where $\widehat{l'}$ is an arbitrary vector which is not aligned with $\hat{l}$.

We can approximate the circle of radius $\overrightarrow{\varepsilon_1}$, around the line by considering a polygon with n vertices centered at origin, and we have:

$$[R_3[c_{\alpha i}, s_{\alpha i}, 0]^t, 0,0,0] \cdot \left(\vec{\delta} + \Delta\vec{x}\right) \leq \overrightarrow{\varepsilon_1}, i = 1, \dots, n$$

and so we can set H and h as:

$$H = \begin{bmatrix} -R_3[c_{\alpha i}, s_{\alpha i}, 0]^t, & 0, & 0, & 0 \\ & \dots & & \\ [R_3[c_{\alpha n}, s_{\alpha n}, 0]^t, & 0, & 0, & 0 \end{bmatrix}, \vec{h} = \begin{bmatrix} -\varepsilon_1 \\ -\varepsilon_1 \\ -\varepsilon_1 \end{bmatrix} - H\vec{\delta} \tag{6}$$

A high value of n means the geometry of the virtual constraint will be closer to the desired shape, but will require a longer computation time.

3.3.1.2 Maintain a Direction

The second virtual fixture, maintaining a direction, is also crucial for the functionality of STRATUS, it requires the tool orientation being close to zeros after each incremental motion. The constraint can be expressed as:

$$\left\|\overrightarrow{\delta_r} + \Delta\overrightarrow{x_r}\right\| \leq \varepsilon_2 \tag{7}$$

where ε_2 is a small positive number for allowable error, the subscript r indicates the rotation components. The matrix form of the linear constraints are then

$$H = \begin{bmatrix} 0, & 0, & 0, & c_{\alpha i}c_{\beta j}, & c_{\alpha i}s_{\beta j}, & s_{\alpha i} \\ & & & \dots & & \\ 0, & 0, & 0, & c_{\alpha i}c_{\beta j}, & c_{\alpha i}s_{\beta j}, & s_{\alpha i} \end{bmatrix}, \vec{h} = \begin{bmatrix} -\varepsilon_1 \\ \dots \\ -\varepsilon_1 \end{bmatrix} - H\vec{\delta} \quad (8)$$

3.3.1.3 Plane Related Constraints

In some scenarios, the tool tip must not penetrate a plane or be confined in a given plane. The closest point on plane can be calculated using:

$$\overrightarrow{\delta_p} = \overrightarrow{x_p} - \overrightarrow{P_{cl}} \quad (9)$$

the geometry constrain is then:

$$\vec{d}^t \cdot \left(\overrightarrow{\delta_p} + \Delta\overrightarrow{x_p}\right) \geq 0 \quad (10)$$

where $\vec{d}^t$is the unit normal direction of the plane and points to the free half space. To confine the tool on the plane, an additional constrain can be added:

$$\vec{d}^t \cdot \left(\overrightarrow{\delta_p} + \Delta\overrightarrow{x_p}\right) \leq \varepsilon_3 \quad (11)$$

where $\varepsilon_3$is a small positive number that defines the error tolerance. Combining the two constrains, the constraints matrices then can then be written as:

$$H = \begin{bmatrix} \hat{d}^t, & 0, & 0, & 0 \\ -\hat{d}^t, & 0, & 0, & 0 \end{bmatrix}, \vec{h} = \begin{bmatrix} 0 \\ -\varepsilon_3 \end{bmatrix} - H\vec{\delta} \quad (12)$$

3.3.2. Virtual Force Method For Virtual Fixture

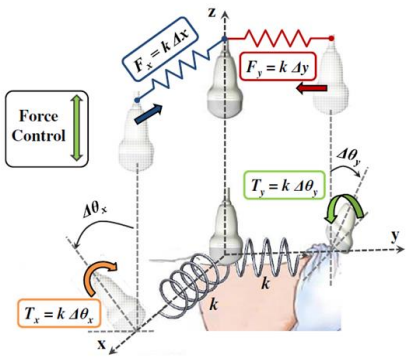

Figure 2. Illustration of virtual spring method for haptic guidance [6]

The second method, error control/virtual spring is mathematically less complex [6][7]. It combines the operating forces with a static virtual force. Static virtual forces act as linear and torsional springs following Hook's law which provide haptic feedback toward a reference US probe position and orientation. Once set, the reference frame will not change until new commands are issued, unlike dynamic virtual forces, which will consistently update its parameters based on real time feedback of the ultrasound images.

The basic mathematical formulation of unconstrained cooperative control with virtual forces is as followed,

$$\begin{bmatrix} \overrightarrow{v_F} \\ \overrightarrow{w_F} \end{bmatrix} = \begin{bmatrix} G_1 & \dots & 0 \\ \vdots & \ddots & \vdots \\ 0 & \dots & G_6 \end{bmatrix} \begin{bmatrix} \overrightarrow{f_F} \\ \overrightarrow{\tau_F} \end{bmatrix} \tag{13}$$

where $\overrightarrow{v_F}$ and $\overrightarrow{w_F}$ are the linear and angular velocity vectors in the force sensor frame, G_n are the elements of the diagonal admittance gain matrix, and $\overrightarrow{f_F}$ and $\overrightarrow{\tau_F}$ are the linear and torsional forces measurements in the force sensor frame. Using nonlinear gains in the system allows the fine motions when the input forces are low and robust movement when higher forces are applied.

An adjoint matrix is computed to convert the velocities from tool frame to world frame as the same in equation 2. Finally, the joint increment command can be

converted from the robot frame velocity using:

$$\dot{\vec{\theta}} = J^{-1}(\vec{\theta}) \cdot \begin{bmatrix} \overrightarrow{v_w} \\ \overrightarrow{w_w} \end{bmatrix} \tag{14}$$

Where $J^{-1}(\vec{\theta})$is the inverse Jacobian matrix as a function of joint positions, and $\dot{\vec{\theta}}$ is the joint increment, the subscript w implies that the velocities are in the world frame.

3.3.2.1. Stay at Point

By applying both a reference position and an orientation, the stay at point virtual fixture is added using this method. The virtual forces and torques are calculated using standard idealized spring model, given by the equation:

$$\begin{bmatrix} \overrightarrow{f_{vf}} \\ \overrightarrow{\tau_{vf}} \end{bmatrix} = \begin{bmatrix} k_x & \dots & 0 \\ \vdots & \ddots & \vdots \\ 0 & \dots & k_{\theta_z} \end{bmatrix} \begin{bmatrix} \overrightarrow{\Delta x} \\ \overrightarrow{\Delta y} \\ \overrightarrow{\Delta z} \\ \Delta\theta_x \\ \Delta\theta_y \\ \Delta\theta_z \end{bmatrix} \tag{15}$$

where $\overrightarrow{\Delta x}$, $\overrightarrow{\Delta y}$ and $\overrightarrow{\Delta z}$ are the linear error from the current tool position to the reference frame, $\Delta\theta_x$, $\Delta\theta_y$ and $\Delta\theta_z$ are the angular error. The diagonal matrix consists of the spring constants for each virtual spring.

Lastly, the complete input force is the sum of both the operator's operating force and the virtual forces.

$$\begin{bmatrix} \overrightarrow{f_F} \\ \overrightarrow{\tau_F} \end{bmatrix} = \begin{bmatrix} \overrightarrow{f_{op}} \\ \overrightarrow{\tau_{op}} \end{bmatrix} + \begin{bmatrix} \overrightarrow{f_{vf}} \\ \overrightarrow{\tau_{vf}} \end{bmatrix} \tag{16}$$

This method can be expanded as error controlled virtual fixture, where the spring stiffness can be tuned up to a high value such that the robot arm will not allow any movement in the wrong direction.

3.3.2.2. Stay on Trajectory

This method also encouraged the development of other forms of virtual constraints. We implemented a stay on a trajectory virtual fixture using gradient increment. For a small a series of points given as the trajectory, a linear search throughout the trajectory is performed during each iteration to find the closest point to the current tooltip. The desired positional increment can be calculated using:

$$\begin{bmatrix} \overrightarrow{v_w} \\ \vec{0} \end{bmatrix} = \begin{bmatrix} \overrightarrow{v_F} \\ \vec{0} \end{bmatrix} \cdot \left(\begin{bmatrix} \overrightarrow{p_{\iota+n}} \\ \vec{0} \end{bmatrix} - \begin{bmatrix} \overrightarrow{x_p} \\ \vec{0} \end{bmatrix} \right) \tag{17}$$

where $\overrightarrow{p_\iota}$ is the current closest point on the trajectory, $\overrightarrow{p_{\iota+n}}$ is the next n point in the trajectory, $\overrightarrow{x_p}$ is the current tool position. The direction of traverse depends on the operator's input force, and thus n can be a negative number. The speed, robustness and finesse of the movement depends on the number of points to skip to calculate the gradient. A low n number can cause the movement speed to decrease but allows fine and precise movements, higher n number allows for faster movement, but it also suggests that certain points in the trajectory will be skipped.

3.4 Synthetic Tracked Aperture Algorithm

We extended the synthetic tracked aperture algorithm (STRATUS) developed by Zhang et al. [8]. The robotic arm is used as a pose tracking device. The imaging coordinate can be calculated through UR5 forward kinematic. By transforming all the US imaging into a consistent reference coordinate, the received US signal can be summed up and produce an US image with larger imaging field and better resolution. The key equations for STRATUS are:

$$p_b = X^{-1} B_b^{-1} B_i X p_i \tag{18}$$

$$RF_b(p_b) = \sum_{i=1}^{N} RF_i(X^{-1} B_b^{-1} B_i X p_i) \tag{19}$$

where p_i is the location vector of i-th pose from the reference coordinate. B_b and B_i are the tracking transformation for the reference imaging coordinate and the i-th pose, respectively. After transforming the poses into reference coordinate, the

received pre-envelope detected radio frequency (RF) signals can be summed up as RF_b.

This algorithm can be applied in both lateral direction (2D STRATUS) and elevational direction (3D STRATUS). 2D STRATUS increases the view and improves the resolution; 3D STRATUS builds up 3D volume for the scanning tissue which could give us an intuitive understanding of the target in three dimensional space. Further, we modify the algorithm to a higher efficiency in order to perform real-time visualization (figure 3). The modified program is three times faster than the previous one.

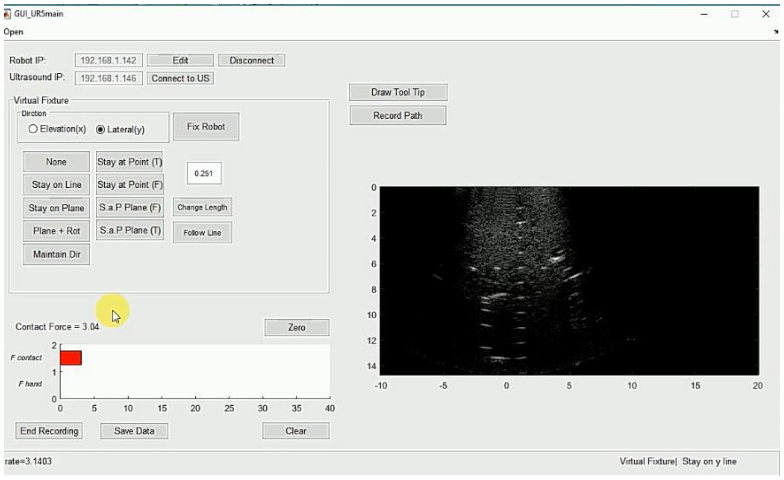

Figure 3. GUI of the system

3.5 Design of 3-axis Load Sensing US Attachment:

We design another US attachment to improve the previous system. The new attachment replaces the 1-DOF load cell with a tri-axis force sensor (FSE 103, Variense, Canada) (Figure 4). This replacement increases the DOF of contact force sensing ability, where the contact force between the US probe and the tissue in three axes is now measurable. The value would reflect in the admittance force control equation (1), and increase the flexibility of the co-robotic US system. It is essential for the system to have a high dexterity for a general clinical use, especially in

echocardiography. The contact force in all direction is important to make the US image reproducible.

Figure 4. Tri-axis force sensor, FSE 103, Variense.

The design of the US attachment is sharing the same connector with the previous design, seen in figure 5. It is consists of a handheld case (outer case) **3**, an inner case **2** and the 3-axis force sensor **1**. The inner and outer case is attached with each other through the force sensor. The shape of the inner case is customized based on the clinical US probe. It can be changed to different inner case for different probe when sharing the same handheld case and the force sensor (Figure 6). Two toggle latches is used for fast detachment/attachment between the connector and the handheld case. This smooth detachment feature makes it easy to change between different US attachment depending on the application

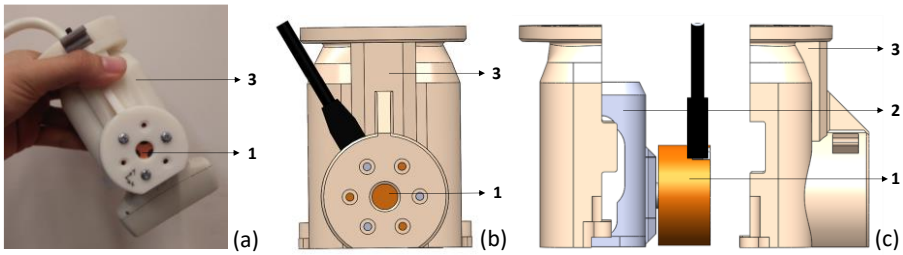

Figure 5. The 3-axis sensing US attachment. **1**: the 3-axis force sensor; **2**: inner case; **3**: handheld case (a) The prototype of the design (b) front view of the design (b) side view of the design


(a)

(b)

Figure 6. The inner case can be changed for different clinical probe attachment while sharing the same handheld case and the force sensor. (a)The inner case used for linear array probe (b) The 3-axis force sensing US attachment applied with linear array probe

4 Experimental and Result

We conducted phantom study, animal and human experiment for system validation. We used the 6+1 DOF force sensing robot system as shown in (figure 1). A clinical convex probe (C5-2 Convex, Ultrasonix) with 128 elements is used for US acquisition. The scanning depth is set to 15 cm and the center frequency was set to 2.0 MHz in all cases. In our project, we only analyzed data for 2D STRATUS, in other words, the data set (200 poses) is collected when the probe moved in pure lateral direction.

4.1 Phantom study

In the phantom study, we scanned a general phantom (figure 7). Figure 8 (a) shows a single slice of the US image before applying STRATUS algorithm. As the distance to the focus point increases, the image resolution decreases and the wire structure becomes defocused. After applying STRATUS (figure 8 (b)), the resolution improved and can be visually observed.

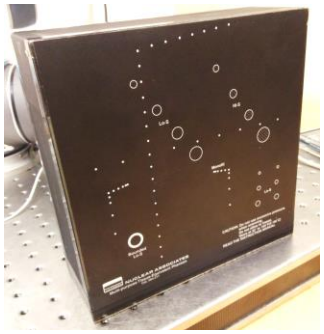

Figure 7. General phantom used for phantom study

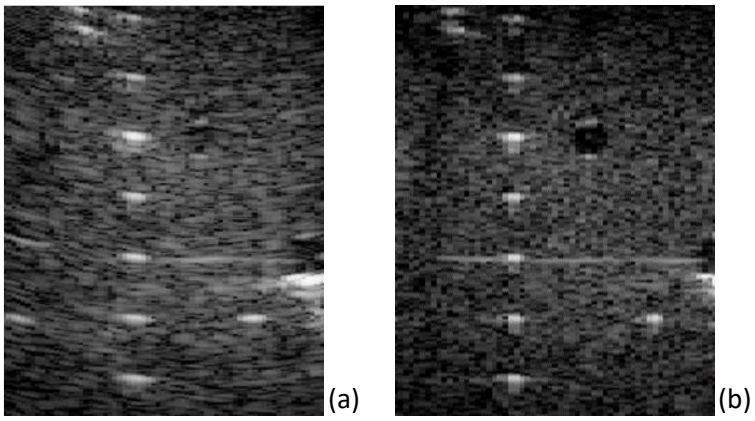

Figure 8. The collected US image of general phantom. (a) Single slice of the data using the synthesizing aperture. (b) The result of STRATUS implementation

4.2 Animal Experiment

In the animal experiment, we performed abdominal scanning of a 105 lb pig in lying position. During the experiment, the pig had a breathing rate around one breath every three seconds. It introduces significant tissue motion and the abdominal structure. Figure 9 (a) shows the recorded contact forces during one scan. The corresponding US image for pose 25 and 30 are shown in Figure 9 (b) and (c) respectively. The tissue motion is obvious and un-negligible. It means that further breath compensation/ motion compensation algorithms should be taken into account before

applying STRATUS.

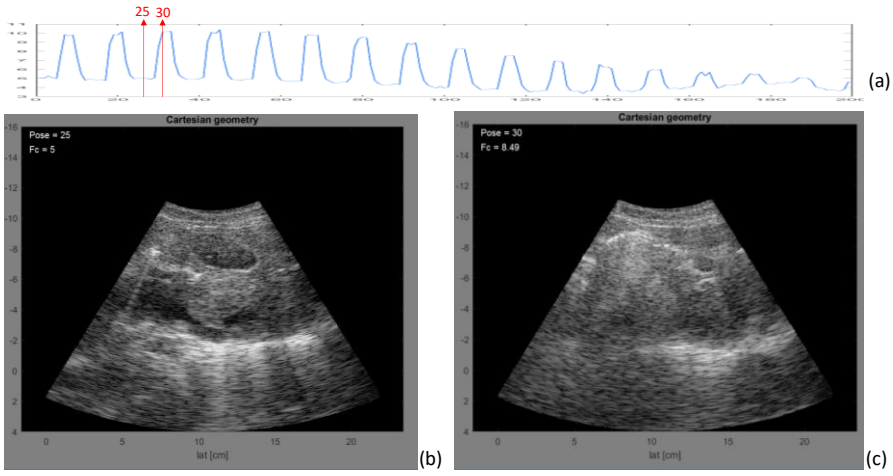

Figure 9. Recorded animal data for one scan. (a) The contact force between the US probe and the pig for 200 poses. (b) The corresponding US image for pose 25th. (c) The corresponding US image for pose 30th.

4.3 Human experiment

To eliminate the effect of tissue motion, we scan the volunteer's tight in a sitting position. Figure 10 (a) shows a single slice of the recorded human leg. Comparing with the single slice, the STRATUS result (Figure 10 (b)) has a larger imaging field.

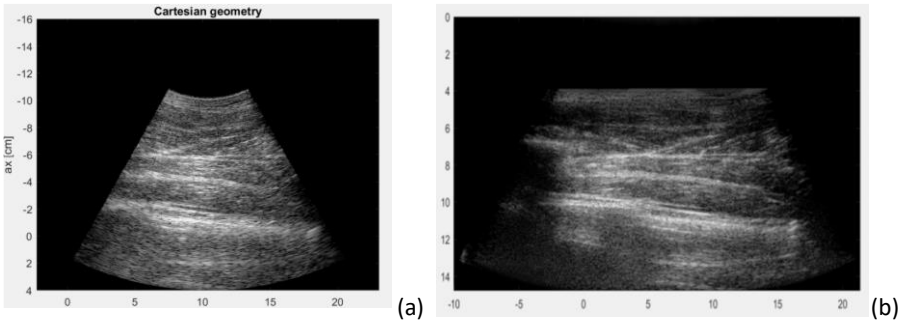

Figure 10. Recorded human leg data for one scan. (a) A single slice of the US image. (b) The

result of STRATUS algorithm implementation

5 Conclusion and Discussion

In this project, we built virtual fixtures using constraint method for cases including stay on line, stay on plane; and virtual string method for error compensation and providing haptic guidance in following a recorded trajectory. We incorporated STRATUS algorithm with the power steering robotic US system and developed real-time data acquisition and visualization for 2D lateral scanning. Phantom study, animal and human experiment were performed to validate the system performance. The result shows that STRATUS works well with with static scanning target but needs modification for object with tissue motion.

To apply STRATUS to moving object, dynamic error compensation should be considered. We could also take advantage of the recorded contact force and perform segmentation to the US data. For example, assuming the tissue deformation is the same with the same contact force, we are able to segment the data into several groups and apply STRATUS separately. More studies need to be addressed according to this issue.

In future development, we would like to extend the dexterity of the system by replacing the 1-DOF force sensing US attachment with the 3-DOF force sensing design. Higher dexterity means the robot can follow user's motion better and brought the procedure more similar to conventional freehand scans; it would be essential for general clinical practice.

Reference

1. Hennersperger C, Fuerst B, Virga S, Zettinig O, Frisch B, Neff T, Navab N (2016) Towards MRI-Based Autonomous Robotic US Acquisitions: A First Feasibility Study. IEEE Transactions on Medical Imaging 1–1. doi: 10.1109/tmi.2016.2620723
2. Şen HT, Cheng A, Ding K, Boctor E, Wong J, Iordachita I, Kazanzides P

(2016) Cooperative Control with Ultrasound Guidance for Radiation Therapy. Frontiers in Robotics and AI. doi: 10.3389/frobt.2016.00049

3. Zhang HK, Cheng A, Bottenus N, Guo X, Trahey GE, Boctor EM (2016) Synthetic tracked aperture ultrasound imaging: design, simulation, and experimental evaluation. Journal of Medical Imaging 3:027001. doi: 10.1117/1.jmi.3.2.027001
4. Fang T-Y, Zhang HK, Finocchi R, Taylor RH, Boctor EM (2017) Force-assisted ultrasound imaging system through dual force sensing and admittance robot control. International Journal of Computer Assisted Radiology and Surgery. doi: 10.1007/s11548-017-1566-9
5. Li M, Kapoor A, Taylor R (2005) A constrained optimization approach to virtual fixtures. 2005 IEEE/RSJ International Conference on Intelligent Robots and Systems. doi: 10.1109/iros.2005.1545420
6. Şen HT, Bell MAL, Iordachita I, Wong J, Kazanzides P (2013) A cooperatively controlled robot for ultrasound monitoring of radiation therapy. 2013 IEEE/RSJ International Conference on Intelligent Robots and Systems. doi: 10.1109/iros.2013.6696791
7. Şen HT, Cheng A, Ding K, Boctor E, Wong J, Iordachita I, Kazanzides P (2016) Cooperative Control with Ultrasound Guidance for Radiation Therapy. Frontiers in Robotics and AI. doi: 10.3389/frobt.2016.00049
8. Zhang HK, Finocchi R, Apkarian K, Boctor EM (2016) Co-robotic synthetic tracked aperture ultrasound imaging with cross-correlation based dynamic error compensation and virtual fixture control. 2016 IEEE International Ultrasonics Symposium (IUS). doi: 10.1109/ultsym.2016.7728522
9. Gilbertson MW, Anthony BW (2013) An ergonomic, instrumented ultrasound probe for 6-axis force/torque measurement. 2013 35th Annual International Conference of the IEEE Engineering in Medicine and Biology Society (EMBC). doi: 10.1109/embc.2013.6609457
10.